

An Investigation Tool for Analyzing Electrostatic Lenses

Hassan N. Al-Obaidi¹ and Ali A. Rashead Al-Azawy²

حسن نوري العبيدي وعلي عبد الامير رشيد العزاوي

**¹Department of Physics, College of Education, Al-Mustansiriyah
University. Corresponding Author E-Mail:hassanmail2006@yahoo.com**

**²Department of Physics, Collage of Science, Karbalaa University.
E-mail:Aliazawy74@yahoo.com**

الخلاصة

تم تقديم أداة تصميم برمجية للعدسات الكهروستاتيكية في هذا العمل. الأداة المعروضة تعمل بالبرنامج الرئيسي المسمى VDTEL، حيث يشير هذا الاختصار إلى أداة تصميم بصرية للعدسات الكهروستاتيكية. تم كتابة البرنامج VDTEL بلغة Visual Basic التي تعمل ضمن مايكروسوفت ستوديو ٢٠١٣ وذلك لاستخدامه بسهولة من قبل مستخدمي الكمبيوتر الذي لا يمتلكون الخبرة باستخدام الحاسوب. وقد تم إرفاق برنامجنا مع برنامج قدم سابقا والذي يقوم بحساب الجهد الكهروستاتيكي للعدسات الكهروستاتيكية. البرنامج الحالي لديه القابلية على حساب الخصائص الشبئية لأي عدسة كهروستاتيكية. وعلاوة على ذلك، للبرنامج القابلية على حساب الخواص الشبئية لأي عدسة مقترحة، ولأكثر من ذلك قابلية الحساب والرسم كل على انفراد او سوية ولأربعة شروط تكبير (انماط تشغيل) هي الصفري، اللانهائي، الواطيء والعالي. مقارنة النتائج تدل بشكل واضح على أن الحسابات ذات تطابق ممتازة يمكن الحصول عليها من برنامج VDTEL لنفس العدسة عند تحليلها مع أي من البرامج الأخرى.

Abstract

A software designing tool for electrostatic lenses is presented in this work. The introduced tool is collected to work under main software named VDTEL, where this abbreviation refers to Visual designing tool for electrostatic lenses. The VDTEL software is written in Visual Basic which works under Microsoft Visual Studio-2013 so as to be used easily even though with a non-genius computer users. The presented software has been attached with previous software which computes the electrostatic potential for electrostatic lenses. The presented software has the ability to compute the objective properties for any electrostatic lens. Furthermore, it may compute and plot together or separately any cardinal element of this lens.

This computation, however, can be executed for each of the well-known four magnification modes, i.e. zero, infinite, low and high magnification conditions.

The comparison results have clearly shows that there is an excellent identical computation which could be obtained from VDTEL software for the same lens when it is analyzed with other counterpart software.

1. Introduction

Indeed, a great importance has been paid for the designing tools of electron lenses during the last four decades. At the time when these tools are coded by means of old procedural programming language, the first decade of this century revealed coding of a tool by means of visual languages. The reasons behind are quit obvious since visual languages supports users by a flexible and easy manipulation for the designs under consideration. Furthermore, they keep time and coast over their counterpart the conventional old languages. It is realizable to announce that designing tools consist of two main steps. First of them aims at finding the electrostatic and/or magnetic imaging field distribution. However, the second one tries to defining the optical properties of this imaging field.

The charged particle beam trajectory is represented by an appropriate mathematical expression such as the polynomial [K. Ahmed 1993; Alani. S 1996]. Or like an n-time differentiable function [Salmeen S. 2002].

Anyway, most of designing tools, in electron optics, that aims at deducing the imaging field are used the technique of finite elements method, [Ives 2000; Chernosvitov 2002; Kalimov 2006 and Munro 2010], finite difference method [Greenfield and Monastyrskii 2009], boundary elements method [Dahl 2000 and Landau 2008], finite integration technique and finite difference time domain methods [Matsuo 2009 and Huang 2009] . While, different numerical methods are adopted to defines the optical properties like Monte Carlo method [Babin 2006 and Zipfel 2006] and Runge Kutta method [Kalvas 2010; Hoang 2010; Humphries 2010 and Holcakova and Marek 2011].

A computer aided design tool is introduced to manipulate magnetic lenses by [Al-Obaidi and Hasan, 2011] and [Al-Saadi, S. R. A. 2007].

Recently an investigation tool has presented to deals with electrostatic lenses [Al-Obaidi and Al-Azawy 2014]. Such tool has adopted the finite elements method to determine electrostatic potential throughout any round electric lens. Present work is put forward to develop this tool such that the objective focal properties for the deduced imaging field can be evaluated.

2. Theoretical Structure

It is well-known that there are two important factors that leads to deteriorate the efficiency of any electron lens, namely spherical and chromatic aberrations. Strictly speaking, the quality of any charged particle optical system depends not only on upon the energy of charge particle but also upon the aberrations. In charged particle optics the spherical aberration is the most important because it limits the resolution of electron microscopes and the smallness of the probes of micro-analyzers. Consequently, such aberration causes blurring in the formed image. Hence, the resolving power of a charged particle optical system being inhibited. The coefficient of spherical aberration referred to the object space C_{S0} is expressed by the following form [Szilagyí 1988]:

$$C_{S0} = \frac{U^{-1/2}(z_0)}{16r_0'^4} \int_{z_0}^{z_1} \left[\left(\frac{5(U''(z))^2}{4(U(z))} + \frac{5(U'(z))^4}{24(U(z))} \right) r^4(z) + \frac{14(U'(z))^3}{3(U(z))} r'(z)r^3(z) - \frac{3(U'(z))^2}{2(U(z))} r'^2(z)r^2(z) \right] \cdot U^{1/2}(z) dz \dots \dots \dots (2-1)$$

As the chromatic aberration is concerned, such defects results from the dependence of the optical parameters of the charged particle lenses on the energy of the focused beam, unlike the case of glass lenses where this effect is not very large and can be corrected to a considerable extent by a judicious choice of the types of glass employed. This aberration coefficient referred to the object space C_{C0} can be expressed by the following integral [Szilagyí 1988].

$$C_{C0} = \frac{U^{1/2}(z_0)}{r_0'^2} \int_{z_0}^{z_1} \left[\frac{1}{2} \left(\frac{U'(z)}{U(z)} \right) r'(z) + \frac{1}{4} \left(\frac{U''(z)}{U(z)} \right) r(z) \right] \frac{r(z)}{U^{1/2}(z)} dz \dots \dots (2-2)$$

Equations (1 and 2) clearly shows that a part from defining the electrostatic potential, the spherical and chromatic aberrations can't being evaluated without finding the electron beam trajectory first. Therefore, to achieve such goal the paraxial ray equation which given by the following expression [Rose 2009] is used;

$$\frac{d^2r}{dz^2} + \frac{U'_0(z)}{2U_0(z)} \frac{dr}{dz} + \frac{U''_0(z)}{4U_0(z)} r = 0 \dots \dots (2-3)$$

This equation is a linear homogeneous second-order differential equation which describes the paths of charge particles moving through a rotationally symmetric electrostatic field that characterized by the potential function $U(z)$. Accordingly, once the axial electrostatic potential has been specified, the first-order properties and so the third-order aberrations can be calculated, by first solving equation (3) for a certain mode of operation.

Consequently, the well-known Runge-Kutta method is used to solve this equation. Accordingly equation (3) needs to be written as follows;

$$r'' = -\frac{U'(z)}{2U(z)} r' - \frac{U''(z)}{4U(z)} r \dots\dots(2-4)$$

Which equivalent to the following mathematical form;

$$r'' = F(z, r, r') \dots\dots(2-5)$$

With initial conditions $r(z_0) = r_0$ and $r'(z_0) = r'_0$ mainly depend on the operated type of magnification. The coefficients of Runge-Kutta method for the electron path (k_i^1) and its correspondent first derivative (k_i^2) are deduced to be as in the following equations respectively;

$$\begin{aligned} k_1^1 &= hr'(z_0) \\ k_1^2 &= hF(z_0, r(z_0), r'(z_0)) \\ k_2^1 &= h(r'(z_0) + \frac{1}{2}k_1^1) \\ k_2^2 &= hF(z_0 + \frac{1}{2}h, r(z_0) + \frac{1}{2}k_1^1, r'(z_0) + \frac{1}{2}k_1^2) \\ k_3^1 &= h(r'(z_0) + \frac{1}{2}k_2^1) \\ k_3^2 &= hF(z_0 + \frac{1}{2}h, r(z_0) + \frac{1}{2}k_2^1, r'(z_0) + \frac{1}{2}k_2^2) \dots\dots\dots(2-6) \\ k_4^1 &= h(r'(z_0) + k_3^1) \\ k_4^2 &= hF(z_0 + \frac{1}{2}h, r(z_0) + k_3^1, r'(z_0) + k_3^2) \end{aligned}$$

Therefore, the coming next values for r and r' can be deduce from the following two recurrence formulas respectively;

$$r(z_0 + h) = r_0 + \frac{1}{6}(k_1^1 + 2k_2^1 + 2k_3^1 + k_4^1) \dots\dots(2-7)$$

$$r'(z_0 + h) = r'_0 + \frac{1}{6}(k_1^2 + 2k_2^2 + 2k_3^2 + k_4^2) \dots\dots(2-8)$$

Where h represent the spacing interval between any two adjacent axial point. Hence the trajectory and its first derivative being determined along the domain of solution, i.e. the lens interval, and so the aberration can be now evaluates.

Anyway, the Simpson's rule is used to estimate the spherical and chromatic aberration integrals shown in equations (1) and 2) respectively. Indeed, both aberration integrals in these two equations can be formulated by the following general form;

$$C = \int_{z_o}^{z_i} F(r, r', U, U', U'') dz \dots (2-9)$$

It is obvious that the axial functions (r, r', U, U', U'') are depend on the axial coordinate z , so it is self-evident that the function F implicitly depend on z . According to the rule of Simpson equation (9) convert to the form below;

$$C = \sum_{z_o+h}^{z_i-h} \frac{h}{3} \left\{ F(r, r', U, U', U'') \Big|_{(z-h)} + 4F(r, r', U, U', U'') \Big|_{(z)} + F(r, r', U, U', U'') \Big|_{(z+h)} \right\} \dots (2-10)$$

Thereby, C_s and C_c have been determined for the hole lens system, i.e. along the interval $z_o \leq z \leq z_i$, by means of the expression shown in equation (10).

It is worth to mention that, the cubic spline differentiation technique has adopted, throughout this work, to implements numerically the derivative for any required function. For example the first and second departure of the potential those are requisite to achieve aberration integrals, see equation (9). However, to keep space it is never clarified in this work and details about this technique can be found in many text books of numerical analysis. Furthermore, the algorithm descript above is coded for programing language by means of visual basic and named visual design tool for electrostatic lenses (SDTEL). However, the coded software will be discussed in the following section.

3. Visual Interfaces

Once the program starts execution, the first page appears as shown in figure.3.1. This page illustrates the name of the software. Pressing the return key makes execution leave the first page to the second one as shown in figure.3.2. The background of this page involves a text information represents the aim of the software and a dialogue box ask user about whether the lens under consideration is symmetric or not. So when the type the lens is assigned in this step, say symmetric for example, user can no longer changes it to the other one, asymmetric in this example, unless truncating execution and start again from the beginning, [Al-Obaidi and Al-Azawy 2014].



Figure.3.1: First page of the VDTEL that appeared just it being starts execution process.

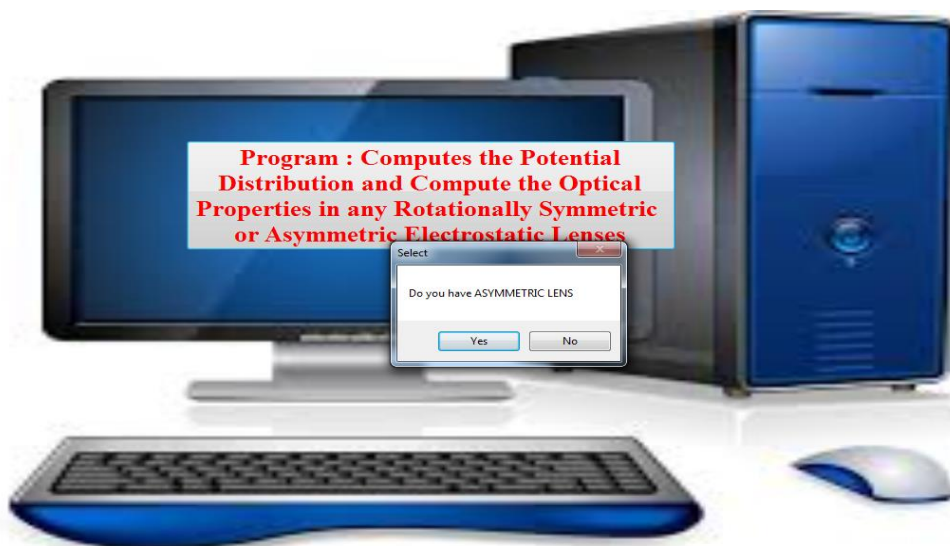


Figure.3.2: Second page of VDTEL.

When the lens type is specified by pressing the bottom (Yes) or (No), execution transit to the forth page of (VDTEL), see figure.3.3a. Actually this page represents the main menu of the software which contain designing, analyzing and documentation options. Construction of these options takes in account that it being similar to that may be found in most of the Microsoft application programs, so as user become familiar to use (VDTEL). The window options: File, Edit, View, Compute, Optical properties Computations, Figures of merit, Plot, Window and About, are shown in figure.3.3 A, in figure.3.3 B, C, D, E, F and G shows the

windows options of Optical properties Computations and Figures of merit respectively.

Figure.3.4 (a, b) shows the profile of the considered lens as it being plotted by VDTEL using the Projection and Mesh Point Lines respectively. It should be mention that, number of these mesh lines can be increased for any assigned reign, especially near the electrode faces. It is well known, however, more number of mesh line are always requested in the action region of electron lenses. Anyway, the distribution these lines are done automatically by VDTEL itself according the input values.

The output results of VDTEL for the axial electrostatic potential, along the optical axis, and the equipotential surfaces throughout the analyzed region that correspond to the asymmetric lens, are plotted in figure.3.5.

A



B

- | optical properties computation |
|--------------------------------|
| Zero magnification |
| Low magnification |
| High magnification |
| Infinite magnification |

C

- | Figures of Merit | Plot | Wind |
|------------------------|------|------|
| Zero magnification | | ▶ |
| Low magnification | | ▶ |
| High magnification | | ▶ |
| Infinite magnification | | ▶ |
| Zero magnification | | ▶ |

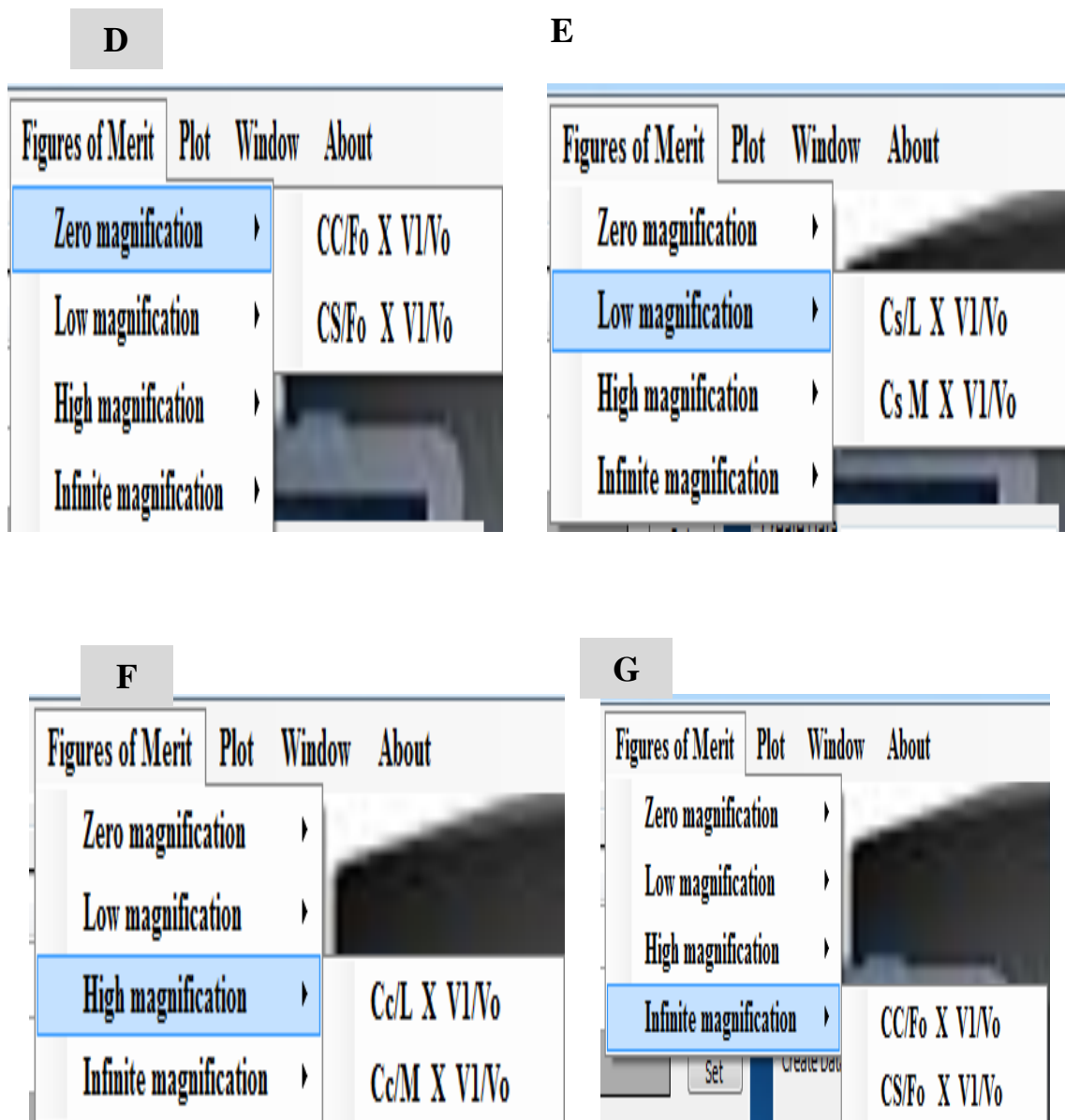
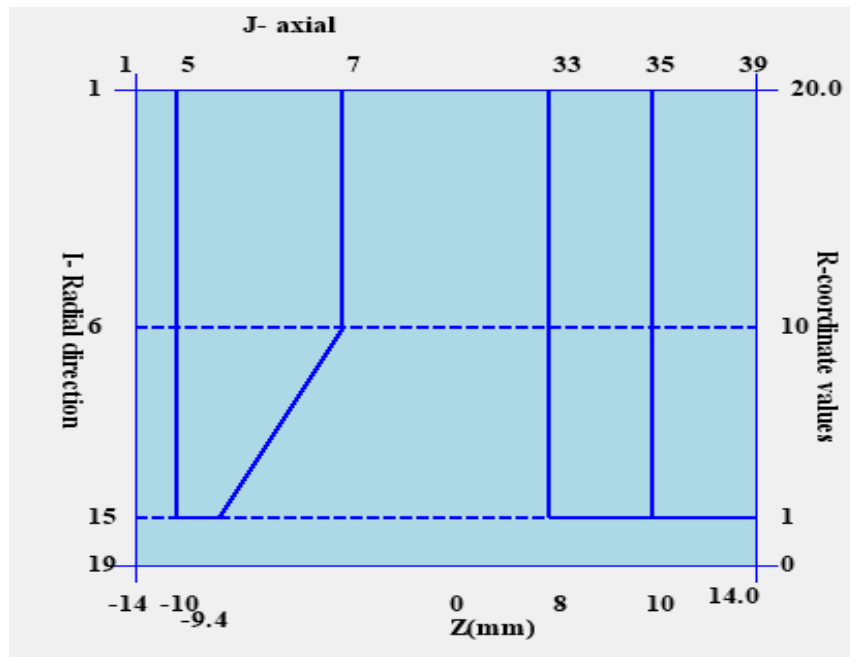
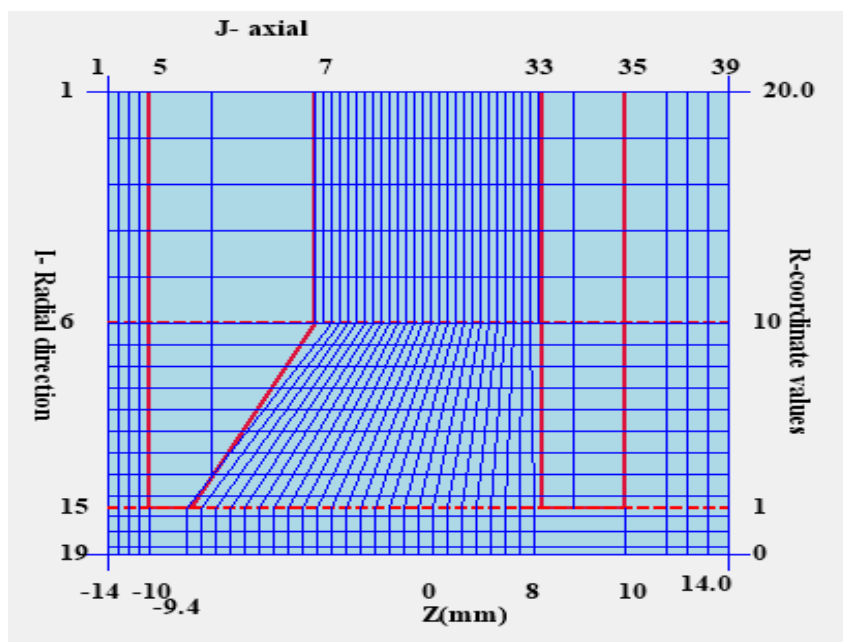


Figure.3.3: A) The Main Menu of (VDTTEL) software. B) Optical Properties Computations. C) Figures of Merit list. D) Zero magnification figures. E) Low magnification figures. F) High magnification figures. G) Infinite magnification figures.

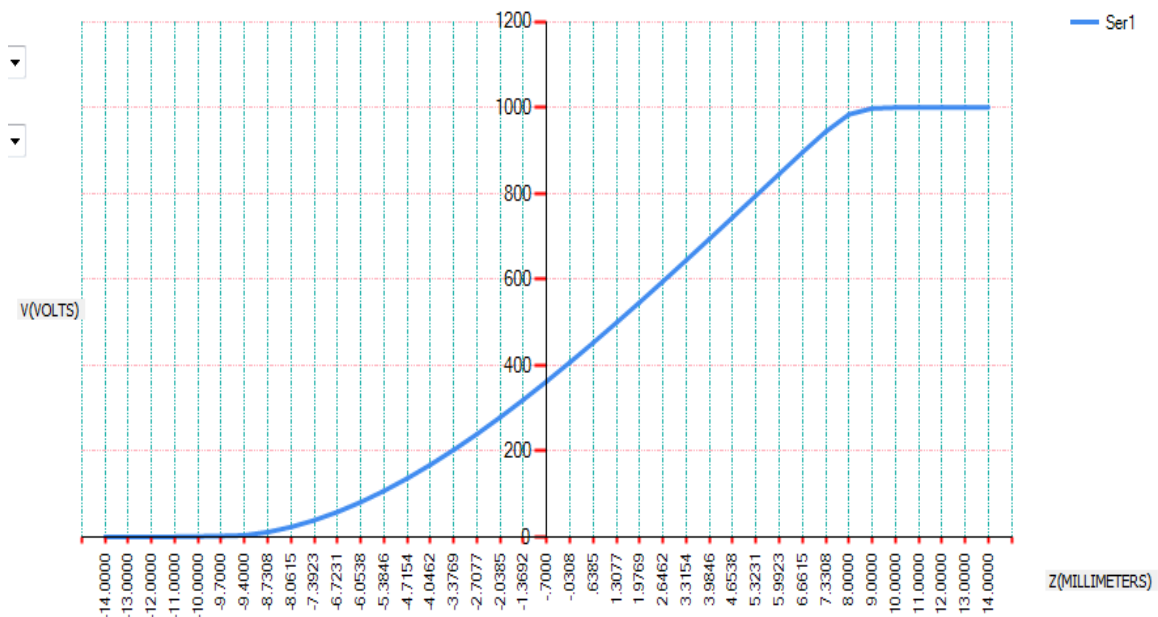


(a)

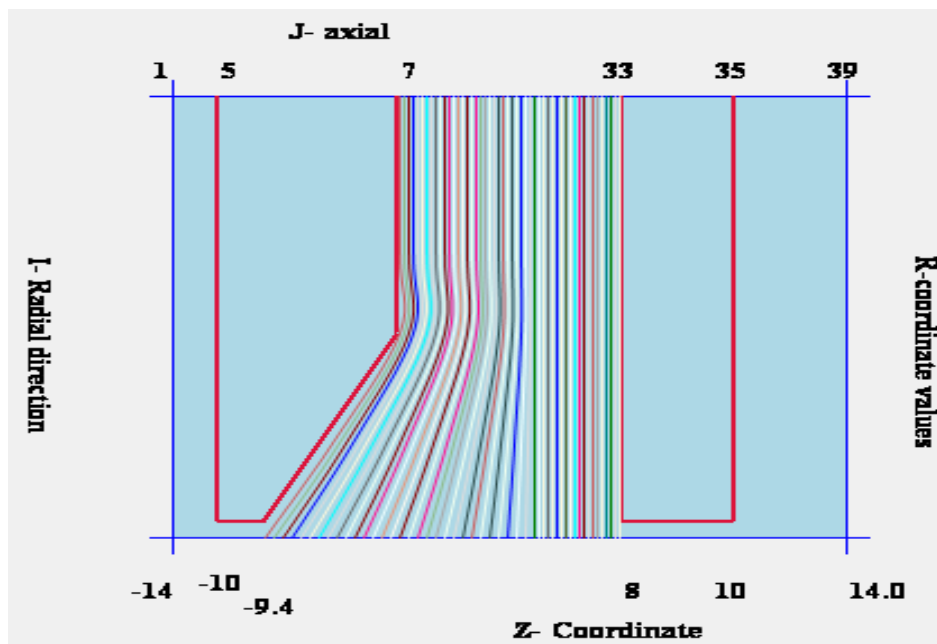


(b)

**Figure.3.4: a) Plot of the mesh projection for asymmetric Munro's lens
b) Distribution of axial and radial mesh lines for asymmetric Munro's lenses.**



(a)



(b)

Figure.3.5: a) the Plot of the deduced axial electrostatic potential distribution for asymmetric case study lenses. b) The equipotential surfaces plotted for asymmetric case study lenses.

4. Typical Computations and Results

In this work the main task of VDTEL is the calculation of the objective focal properties for the lens under consideration. These focal properties are; the spherical aberration coefficient (C_S), chromatic aberration coefficient (C_C), objective focal length (f_o), object plane (z_o), image plane (z_I) and magnification (M). Furthermore, VDTEL has been supplied to deduce several figures of merit that are necessary for researchers and designers to find out the optimum lens. For example the relative spherical aberration (C_S/ f_o), relative chromatic aberration (C_C/ f_o) can be computed and / or plotted by VDTEL software for electrostatic asymmetric lens. Keep in mind that, these parameters can be determined for any of the zero, infinite, low and high magnification conditions.

Some of these objective focal properties that are belong to the asymmetric case study lenses which are published by [Munro, 1975] are listed in table.4.1. Indeed, they are computed by VDTEL for the case of zero magnification condition, as an example. Here also one can find an excellent agreement between the results of present work and those counterpart of [Munro, 1975]. For more clarity, the f_o , C_S and C_C are calculated by VDTEL as a function of the parameter V_I/V_O for the considered lens. However, the results are listed, together with that of Munro's procedure for comparison, in table.4.2 for asymmetric lens. The excellent identical between the two groups of results is obvious.

Table.4.1: The objective focal properties for asymmetric case study lens at zero magnification condition.

OBJ.SIDE VOLTAGE V ₀ (VOLT)	IM.SIDE VOLTAGE V ₁ (VOLT)	IMAGE PLANE Z ₁ (mm)	PRINC PLANE Z _P (mm)	FOCAL LENGTH f ₀ (mm)	SPHER. AB. C _S (mm)	CHROM. AB. C _C (mm)
1000	10000	15.42	-18.44	33.86	400.21	163.54
1000	20000	6.24	-18.34	24.58	236.58	185.61
1000	30000	2.77	-18.78	21.55	206.23	218.44
1000	40000	0.76	-19.25	20.01	197.56	252.87
1000	50000	-0.61	-19.69	19.08	196.04	287.57
2000	10000	35.80	-20.62	56.42	1336.02	189.92
2000	20000	15.42	-18.44	33.86	400.21	163.54
2000	30000	9.380	-18.22	27.61	279.07	171.54
2000	40000	6.24	-18.34	24.58	236.58	185.61
2000	50000	4.22	-18.54	22.76	216.69	201.63

Table.4.2: Some of the objective focal properties for the asymmetric case study lens computed by VDTEL for the zero magnification condition.

<u>V₁/V₀</u>	<u>f₀(mm)</u>		<u>C_S(mm)</u>		<u>C_C(mm)</u>	
	<u>Munro</u>	<u>VDTEL</u>	<u>Munro</u>	<u>VDTEL</u>	<u>Munro</u>	<u>VDTEL</u>
5	56.42	56.92	1336.02	1337.20	189.92	188.21
10	33.86	33.90	400.21	401.61	163.54	164.50
15	27.61	27.34	279.07	278.27	171.54	172.94
20	24.58	24.87	236.58	238.38	185.61	186.81
25	22.76	22.94	216.69	217.29	201.63	202.93
30	21.55	21.80	206.23	209.43	218.44	219.64
40	20.01	20.99	197.56	198.66	252.87	254.97
50	19.08	19.88	196.04	197.40	287.57	289.87

In a way similar to that presented in table.4.1 the objective focal properties for the asymmetric case study lenses are shown in tables.4.3, 4 and 5 respectively. Actually, the same remarks that could be extracted for the zero magnification mode can be write down for low, high and infinite magnification modes. This results clearly indicate that the software VDTEL can be used to investigates, with same characteristic, electrostatic lens for all of the sorts of magnification types.

For further objective comparison, results of these types of magnifications are listed together with the correspondence ones that published in [Munro, 1975]. Anyway, these results are tabulated in tables.4.6, 7 and 8 for low, high and infinite magnification conditions respectively for the case study lens. These results give again an evidence for the ability of VDTEL to analyze electrostatic lens at different magnification modes.

Table.4.3: The objective focal properties for asymmetric case study lens at low magnification condition.

OBJ.SIDE VOLTAGE V ₀ (VOLT)	IM.SIDE VOLTAGE V _I (VOLT)	Object PLANE Z ₀ (MM)	Image PLANE Z _I (MM)	Mag. M	SPHER. AB. C _s (MM)	CHROM. AB. C _c (MM)
1000	10000	-500	16.18	0.02238	449.69	174.96
1000	10000	-1000	15.79	0.01094	423.84	169.07
1000	20000	-500	6.52	0.01134	250.68	192.22
1000	20000	-1000	6.38	0.00558	243.44	188.85
1000	30000	-500	2.94	0.00808	214.67	223.86
1000	30000	-1000	2.86	0.00399	210.36	221.10
1000	40000	-500	0.89	0.00649	203.83	257.78
1000	40000	-1000	0.83	0.00320	200.64	255.29
1000	50000	-500	-0.51	0.00553	201.17	292.20
1000	50000	-1000	-0.56	0.00273	198.56	289.85
2000	10000	-500	38.89	0.05476	1775.91	220.61
2000	10000	-1000	37.28	0.02626	1534.96	204.35
2000	20000	-500	16.18	0.02239	449.69	174.96
2000	20000	-1000	15.79	0.01094	423.84	169.07
2000	30000	-500	9.79	0.01476	301.19	179.53
2000	30000	-1000	9.58	0.00725	289.77	175.44
2000	40000	-500	6.52	0.01134	250.68	192.22
2000	40000	-1000	6.38	0.00558	243.44	188.85
2000	50000	-500	4.43	0.00937	227.16	207.51
2000	50000	-1000	4.32	0.00462	221.80	204.52

Table.4.4: The objective focal properties for asymmetric case study lens at high magnification condition.

OBJ.SIDE VOLTAGE V_O (VOLT)	IM.SIDE VOLTAGE V_I (VOLT)	Object PLANE Z_O (MM)	Image PLANE Z_I (MM)	Mag. M	SPHER. AB. C_S (MM)	CHROM. AB. C_C (MM)
1000	10000	-22.40	500	14.319	67.29	13.80
1000	10000	-22.02	1000	29.094	61.94	13.22
1000	20000	-15.52	500	20.103	14.25	5.86
1000	20000	-15.39	1000	40.460	13.51	5.70
1000	30000	-13.53	500	23.091	6.92	3.74
1000	30000	-13.44	1000	46.312	6.63	3.65
1000	40000	-12.57	500	24.965	4.39	2.76
1000	40000	-12.51	1000	49.968	4.23	2.70
1000	50000	-12.01	500	26.254	3.17	2.20
1000	50000	-11.96	1000	52.476	3.06	2.15
2000	10000	-42.24	500	8.232	656.99	40.75
2000	10000	-40.65	1000	17.098	560.26	37.52
2000	20000	-22.40	500	14.319	67.29	13.80
2000	20000	-22.02	1000	29.094	61.94	13.22
2000	30000	-17.65	500	17.784	25.60	8.22
2000	30000	-17.45	1000	35.907	24.04	7.95
2000	40000	-15.52	500	20.103	14.25	5.86
2000	40000	-15.39	1000	40.460	13.51	5.70
2000	50000	-14.31	500	21.794	9.45	4.57
2000	50000	-14.21	1000	43.773	9.01	4.45

Table.4.5: The objective focal properties for asymmetric case study lens at infinite magnification condition.

OBJ.SIDE VOLTAGE V_o (VOLT)	IM.SIDE VOLTAGE V_i (VOLT)	Object PLANE Z_o (MM)	PRINC PLANE Z_p (MM)	FOCAL LENGTH f_0 (MM)	SPHER. AB. C_s (MM)	CHROM. AB. C_c (MM)
1000	10000	-21.65	-10.95	10.70	57.10	12.67
1000	20000	-15.25	-9.76	5.49	12.81	5.54
1000	30000	-13.36	-9.43	3.93	6.34	3.57
1000	40000	-12.45	-9.28	3.16	4.07	2.64
1000	50000	-11.91	-9.21	2.70	2.95	2.11
2000	10000	-39.17	-13.95	25.22	480.77	34.64
2000	20000	-21.65	-10.95	10.70	57.10	12.67
2000	30000	-17.25	-10.13	7.12	22.58	7.70
2000	40000	-15.25	-9.76	5.49	12.81	5.54
2000	50000	-14.10	-9.55	4.55	8.60	4.33

Table.4.6: Some of the objective focal properties for the asymmetric case study lens computed by VDTEL for the low magnification condition at an object position $z_o=-500$ mm.

V_i/V_o	<u>M</u>		<u>C_s (mm)</u>		<u>C_c (mm)</u>	
	Munro	VDTEL	Munro	VDTEL	Munro	VDTEL
5	0.05476	0.05665	1775.91	1723.10	220.61	165.53
10	0.02239	0.02883	449.69	465.60	174.96	170.41
15	0.01476	0.01778	301.19	311.90	179.53	178.26
20	0.01134	0.01227	250.68	259.08	192.22	189.51
25	0.00937	0.00996	227.16	220.15	207.51	201.16
30	0.00808	0.00656	214.67	200.48	223.66	222.36
40	0.00649	0.00597	203.83	199.76	257.78	259.26
50	0.00553	0.00497	201.17	200.27	292.20	289.21

Table.4.7: Some of the objective focal properties for the asymmetric case study lens computed by VDTEL for the high magnification condition at an image position $z_I=500\text{mm}$.

<u>V_I/V_O</u>	<u>M</u>		<u>$C_S(\text{mm})$</u>		<u>$C_C(\text{mm})$</u>	
	<u>Munro</u>	<u>VDTEL</u>	<u>Munro</u>	<u>VDTEL</u>	<u>Munro</u>	<u>VDTEL</u>
5	8.232	8.233	656.99	655.09	40.75	40.84
10	14.319	14.318	67.29	67.34	13.80	13.76
15	17.784	17.785	25.60	25.89	8.22	8.39
20	20.103	20.104	14.25	14.37	5.86	5.77
25	21.794	21.795	9.45	9.51	4.57	4.61
30	23.091	23.090	6.92	6.88	3.74	3.70
40	24.965	24.966	4.39	4.29	2.76	2.68
50	26.254	26.255	3.17	3.12	2.20	2.18

Table.4.8: Some of the objective focal properties for the asymmetric case study lens computed by VDTEL for the infinite magnification condition.

<u>V_I/V_O</u>	<u>$f_0(\text{mm})$</u>		<u>$C_S(\text{mm})$</u>		<u>$C_C(\text{mm})$</u>	
	<u>Munro</u>	<u>VDTEL</u>	<u>Munro</u>	<u>VDTEL</u>	<u>Munro</u>	<u>VDTEL</u>
5	25.22	25.22	480.77	480.73	34.64	34.63
10	10.70	10.71	57.10	57.11	12.67	12.69
15	7.12	7.13	22.58	22.56	7.70	7.72
20	5.49	5.47	12.81	12.82	5.54	5.55
25	4.55	4.56	8.60	8.61	4.33	4.32
30	3.93	3.95	6.34	6.33	3.57	3.56
40	3.16	3.15	4.07	4.08	2.64	2.63
50	2.70	2.71	2.95	2.96	2.11	2.10

Concerning with the low and high magnification conditions, the positions of the image and object are an important parameters in defining the objective focal properties. Obviously, these two positions affects the height and slope of the beam trajectory at the entrance and exit apertures of the objective lens respectively. So, it is important to verify the results of VDTEL program when these parameters being varied. Consequently, the real values of z_I and z_o are changed from 500 mm to 1000 mm and comparison results of table.4.6 from one hand and table.4.7 from another one, are repeated again. However, the new results are presented in tables.4.9 and 10 respectively.

It seen that, the agreement between the results VDTEL software and the conventional procedure is still fulfilled. Thereby, this is another credit to the benefit of the algorithm followed in his work. On the other hand, the increases of the object position by twice amount has led to reducing the magnification almost to its half value for the low magnification, while it cause to approximately doubling of the magnification for high magnification mode. This, in fact, is a direct consequence for the reduction of the angular departure of electron beam as it inter, and exit, the field of the lens for low, and high, magnification respectively. In other word, the positioning of an object away from the lens make the interaction between the electron beam and electric field smoothly come to happened. Thus, disturbance in the motion of electron becomes less strong when the object position situated away from the lens edge. This in turn, however, lead to enhancing the aberration coefficients especially for low values of the quotient V_I/V_O .

Table.4.9: Some of the objective focal properties for the asymmetric case study lens computed by VDTEL for the low magnification condition at an object position $z_o=-1000$ mm.

<u>V_I/V_O</u>	<u>M</u>		<u>C_s(mm)</u>		<u>C_c(mm)</u>	
	<u>Munro</u>	<u>VDTEL</u>	<u>Munro</u>	<u>VDTEL</u>	<u>Munro</u>	<u>VDTEL</u>
5	0.02626	0.02428	1534.69	1545.60	204.35	209.05
10	0.01094	0.01048	423.84	431.57	169.07	161.32
15	0.00725	0.00701	289.77	290.04	175.44	170.82
20	0.00558	0.00541	243.44	240.07	188.85	184.50
25	0.00462	0.00449	221.80	219.81	204.52	200.85
30	0.00399	0.00388	210.36	208.27	221.10	219.86
40	0.00320	0.00313	200.64	199.61	255.29	250.53
50	0.00273	0.00267	198.56	195.62	289.85	285.36

Table.4.10: Some of the objective focal properties for the symmetric case study lens computed by VDTEL for the high magnification condition at an image position $z_I=1000\text{mm}$.

<u>V_I/V_O</u>	<u>M</u>		<u>$C_S(\text{mm})$</u>		<u>$C_C(\text{mm})$</u>	
	<u>Munro</u>	<u>VDTEL</u>	<u>Munro</u>	<u>VDTEL</u>	<u>Munro</u>	<u>VDTEL</u>
5	17.098	17.099	560.26	560.27	37.52	37.53
10	29.094	29.093	61.94	61.93	13.22	13.23
15	35.907	35.906	24.04	24.05	7.95	7.96
20	40.460	40.461	13.51	13.52	5.70	5.70
25	43.773	43.772	9.01	9.02	4.45	4.45
30	46.312	46.313	6.63	6.64	3.65	3.66
40	49.968	49.969	4.23	4.22	2.70	2.70
50	52.476	52.478	3.06	3.08	2.15	2.16

5. Figures of Merit

The VDTEL has been supported to print out and/or plot several figures of merit that one usually needs to achieve an optimum lens design. A typical example for these results are; C_S/f_o , C_C/f_o , C_S/C_C , C_S/L , C_C/L , $C_S M$, $C_C M$, C_S/M , C_C/M and M as a function of V_I/V_O . Some of these figures, indeed, concern one or two modes of magnifications, while others are interested to all of the magnifications. For example figures.5.1 and 2 shows output windows for VDTEL that reveal the relative chromatic and the relative spherical aberration as a function of the image to object potential quotient respectively, for the asymmetric case study lens at the zero magnification condition. It is seen that, this figure shows both of the tabulated data and its corresponding curve for C_C/f_o versus V_I/V_O . Thereby, the user can directly decide that the considered lens don't serve a short projection distances concerning the chromatic aberration coefficient, while its suitable for the spherical aberration coefficient. In other word, the considered lens is more appropriated to test solid samples while its improper to examine biological ones.

Furthermore, figures.5.3 and 4 reveal the same figures of merit mentioned previously with the same considered lens but for the infinite magnification condition. It is quite obvious that the asymmetrical case study lens for this type of operating mode can be used to analyze both solid and biological samples in contract to the zero magnification. Anyway, figures.5.5, 6, 7 and 8 shows a nether output result window for VDTEL which reveal the magnified C_C and C_S for the case study lens at low and high magnification conditions asymmetric lens. One can directly predict

that, a part from the changes in magnification the objective aberration coefficients enhanced as long as the potential at the image side increases.

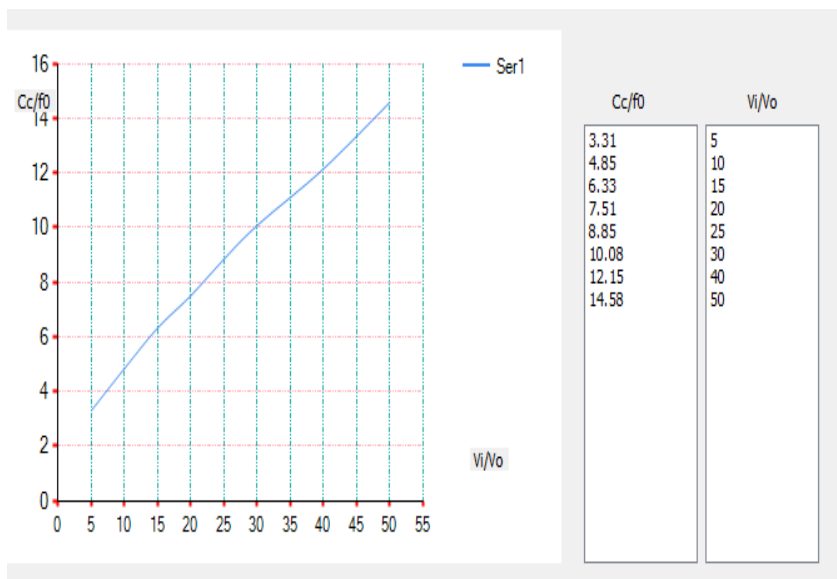


Figure.5.1: The relative chromatic aberration C_c/f_0 as a function of parameter V_i/V_o for asymmetric case study lens at zero magnification condition.

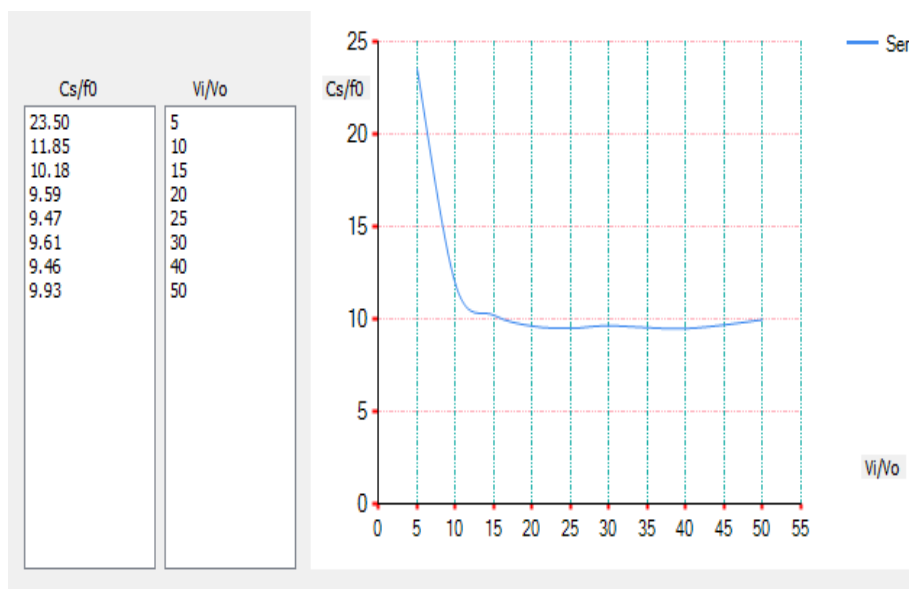


Figure.5.2: The relative spherical aberration C_s/f_0 as a function of parameter V_i/V_o for asymmetric case study lens at zero magnification condition.

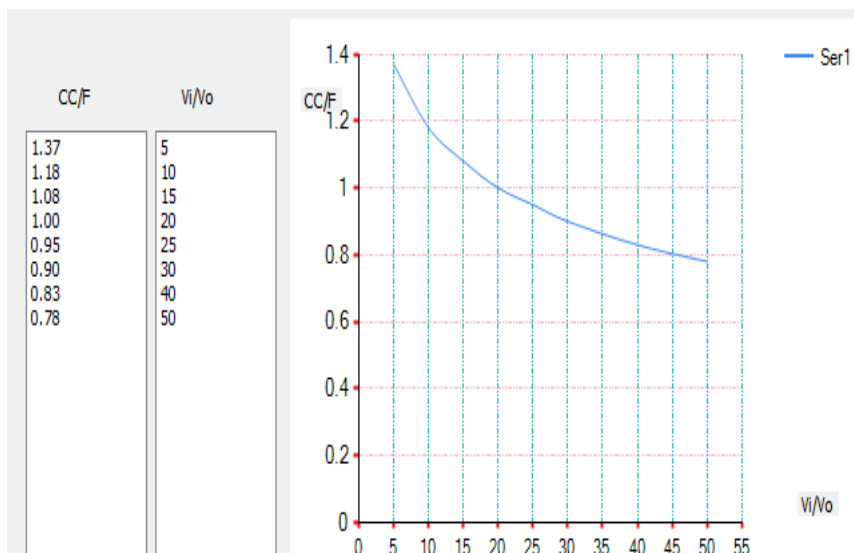


Figure.5.3: The relative chromatic aberration C_C/f_0 as a function of parameter V_I / V_O for asymmetric case study lens at infinite magnification condition.

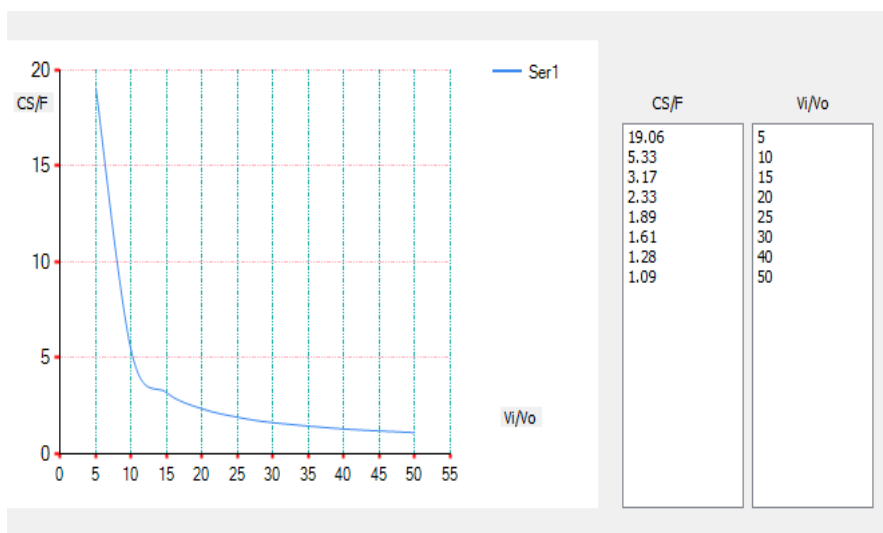


Figure.5.4: The relative spherical aberration C_S/f_0 as a function of parameter V_I / V_O for asymmetric case study lens at infinite magnification condition

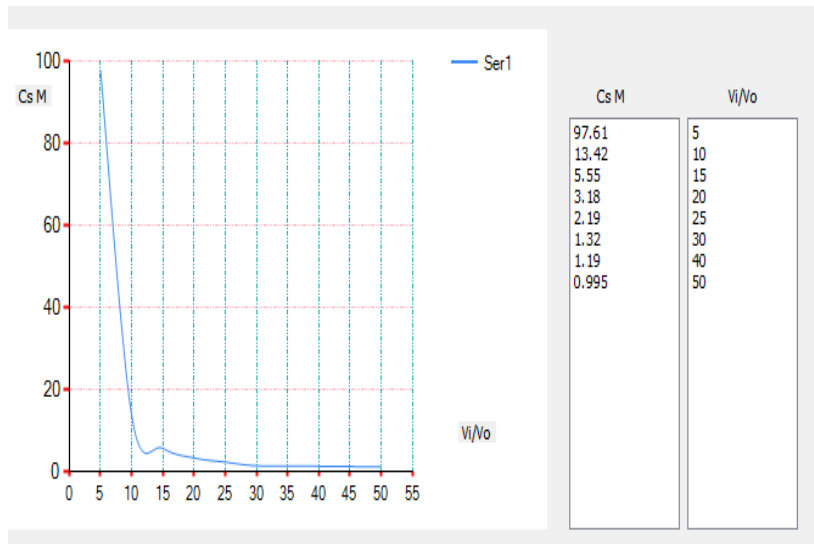


Figure.5.5: The quantity $C_s M$ versus the parameter V_I / V_O for asymmetric case study lens at low magnification condition when $z_0=-500$.

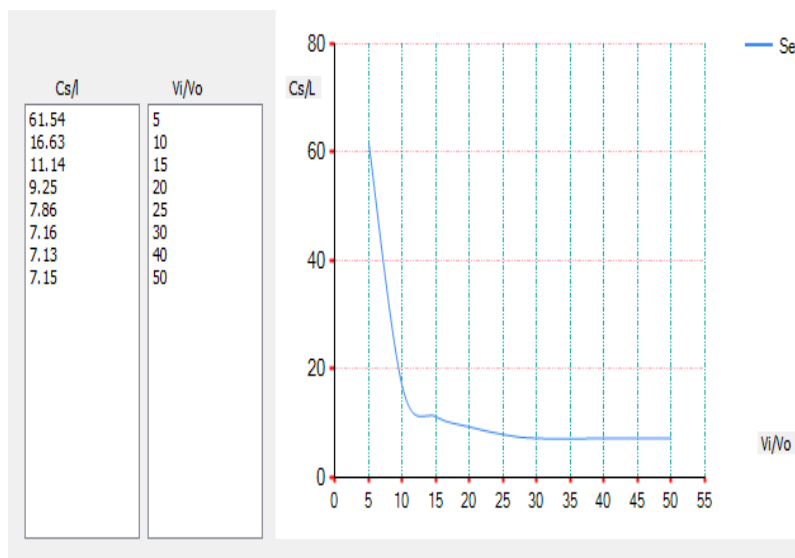


Figure.5.6: The quantity C_s/L versus the parameter V_I / V_O for asymmetric case study lens at low magnification condition when $z_0=-500$.

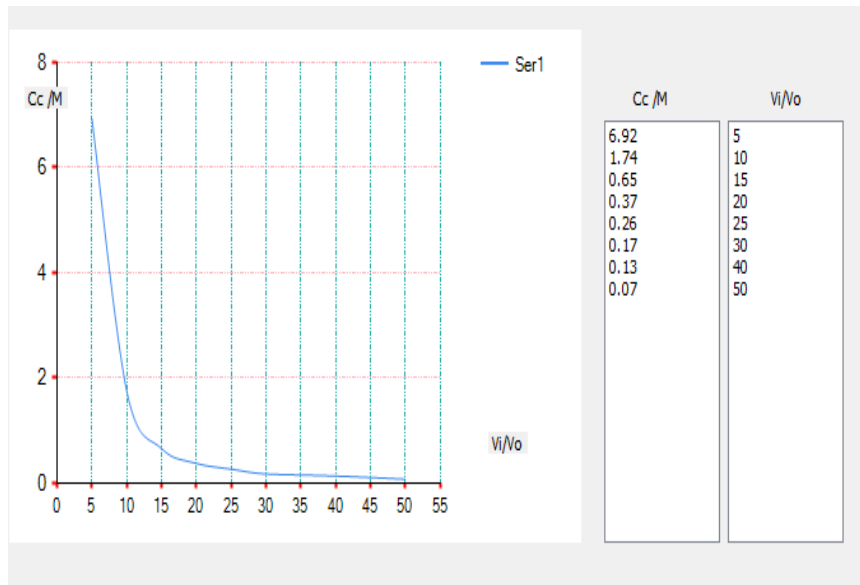


Figure.5.7: The quantity C_c /M versus the parameter V_I / V_O for asymmetric case study lens at high magnification condition when $z_I=500$.

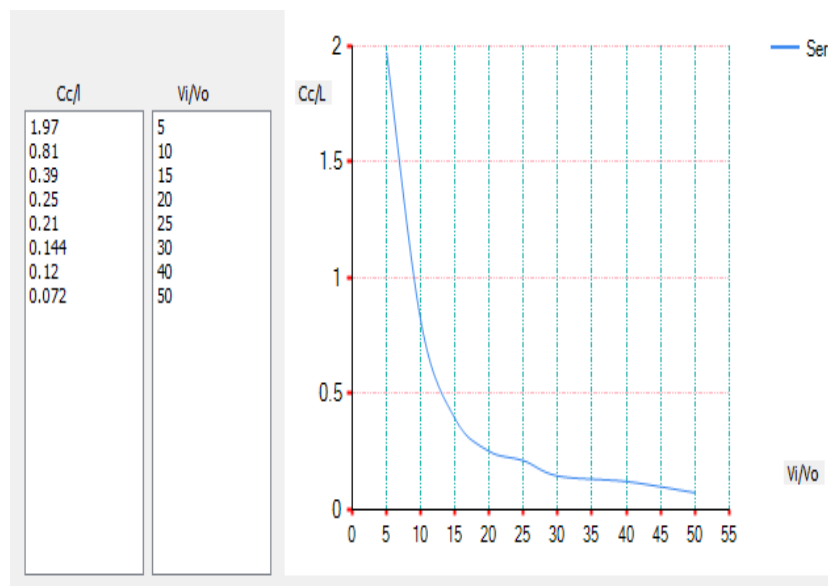


Figure.5.8: The quantity C_c /L versus the parameter V_I / V_O for asymmetric case study lens at high magnification condition when $z_I=500$.

Another example for the VDTEL output results windows are presented in figures.5.9 and 10. These figures show the variation of magnification as a function of the quotient V_I / V_O for asymmetric case study lens at high

and low modes respectively. It is clear that the increases of the potential in the image side cause an increase for M at the high magnification condition. While it cause a decreases for M at the low magnification mode.

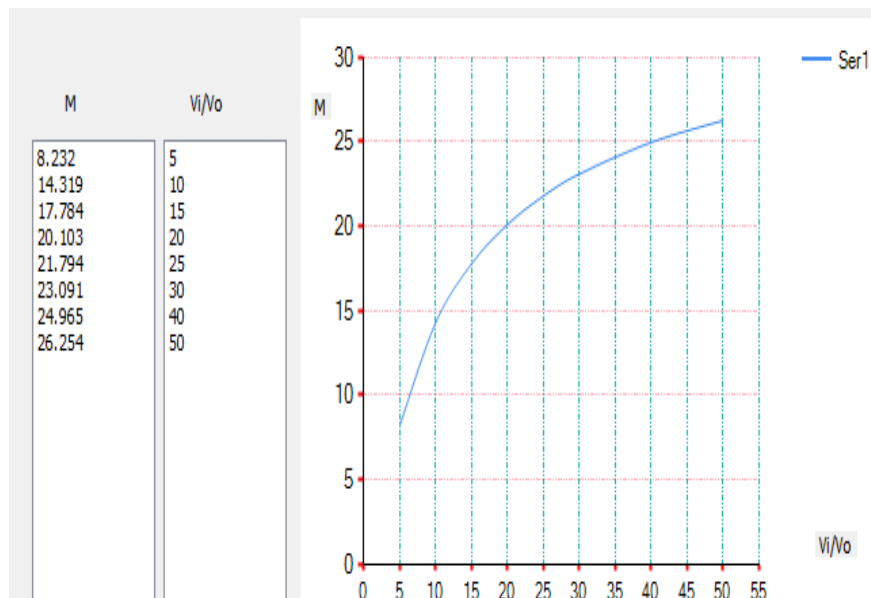


Figure.5.9: The magnification M as a function of parameter V_I / V_O for asymmetric case study lens at high magnification condition when $z_I = 500\text{mm}$.

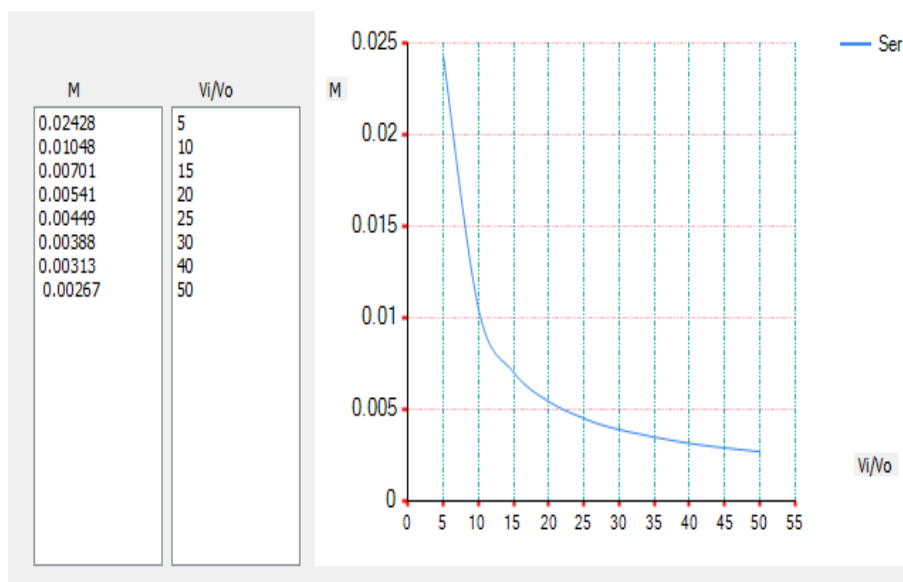


Figure.5.10: The magnification M as a function of parameter V_I / V_O for asymmetric case study lens at low magnification condition when $z_O = -500\text{mm}$.

6. Conclusions

The introduced designing software can be used to investigate electrostatic lenses effectively by means of the analysis procedure. All the categories of electrostatic lenses can be easily analyzed with the aid the VDTEL. The VDTEL software provide users and researchers the opportunity to gets many (data and figures) of merit for many different applications. Furthermore the comparison proved that an accurate result may obtain from the designed software. The used visual programming language gives raise for further realization of investigation concerning electrostatic asymmetric lenses. (VDTEL) may widely be used by non-expert users because it involve on adopting interfaces of direct indications.

References

- Al-Ani S. K. (1996). "*A Computational Study of Space-Charge Effect on the Design of Electrostatic Lenses*" Ph.D Thesis Al-Nahrain University, Baghdad, Iraq.
- Al-Obaidi, H. N.A. and Al-Azawy A. (2014) "*Visual Design Tool for Electrostatic Lenses*" , Journal of Advances in physics, Vol. 5, No.2.
- Al-Obaidi H.N. and Hasan H.S., (2011), "**Computer Aided Design Tool For Electron Lenses(CATEL)**", Proc.18th.Conf. Col. Educe., Al-Mustansiriyah University, 20-21 apr 2011, special No.74.
- Al-Saadi, S. R. A. (2007), "**Improvement in Application of The Theory of Charged Beam Optics**", Ph.D.Thesis, Al-Mustansiriyah University, Iraq.
- Babin , S. (2006), "*CHRIOT Software Tool to Model SEM Signal and Electron Scattering in Targets*", Seventh International Conference on Charged Particle Optics (CPO-7), Abstract for Computer Software Demonstrations, Trinity College Junior Parlour.
- Chernosvitov, A. , Kalimov, A. and Wollnik, H. (2002), "*Design of an iron dominated quadrupole magnet with a high pole-tip flux density*", IEEE Trans. Appl. Supercond., vol.12, pp.1430–1433.
- Dahl, D. A. (2000), "*SIMION for personal computer in reflection*", Int. J. Mass Spectrom. 200, pp. 3-25.
- Greenfield, D. and Monastyrskii, M. (2009), "*Advance in Imaging and Electron Physics*", 1st ed., (London: Academic Press).
- Hoang, H. Q. , Osterberg, M. and Khursheed, A. (2010), "*Electron Optics Simulation Software at NUS*", Eighth International Conference on Charged Particle Optics (CPO-8) – Conference Handbook, Suntec City Convention Centre, Singapore.
- Holcakova, R. and Marek, M. (2011), "*Innovative research in electron microscopes, analysis of magnetic field distribution of some types of magnetic lenses by FEM*", 10th International Conference on Environment and Electrical Engineering , pp.1-4, IEEE Journals.
- Huang, T. , Hu, Q. , Yang, Z. , Li, B. , Li, J. Q. , Jin, X. L. , Hu, Y. L. , Zhu, X. F. ,
- Humphries, S. (2011), "*Three-dimensional Charged-particle Optics and Gun Design*", Field Precision LLC, CRC Press, Albuquerque, New Mexico U.S.A.
- Ives, L. , Bui, T. , Vogler W. and Cendes Z. (2000), "*BOA - a Finite Element Charged Particle Code with Adaptive, Finite Element Meshing*", Vacuum Electronics Conference, p.2 , IEEE Journals.
- K. Ahmad. (1993), "*Computerized Investigation on the Optimum Design and Properties of Electrostatic lens*", Ph.D thesis Al-Nahrain University, Baghdad, Iraq.

- Kalvas, T. , Tarvainen, O. , Ropponen, T. , Steczkiewicz, O. and Ärje, J. (2010), "***IBSIMU - A Three-Dimensional Simulation Software for Charged Particle Optics***", Review of Scientific Instruments, Volume 81, Issue 2.
- Kalimov, A. , Potienko, A. and Wollnik, H. (2006), "***Optimization of the Pole Shape of Quadrupole Magnets by MULTIMAG***", IEEE Transactions On Applied Superconductivity, Vol.16, NO.2.
- Landau, R. H. (2008), "***A Survey Of Computational Physics***", Princeton University PREEES.
- Matsuo, T. (2009), "***Preliminary Study of Electromagnetic Field Computation on a Space-Time Grid***", Kyoto University, Japan.
- Munro, E. (1975), "***A Set of Computer Programs for Calculating of Properties Electron Lenses***", Univ. of Cambridge, Depart. Of Eng. Report CUED/B- Elect. TR 45.
- Munro, E. (2010), "***Munro's Electron Beam Software – Software Catalogue*** ", MEBS Ltd.
- Rose, H. (2009), "***Geometrical Charged-Particle Optics***" Springer Series In Optical Sciences.
- Salmeen S. J. (2002), "***Computer Aided-Synthesis of Electron Using A Preassigned Analytical Functions***" M.Sc. Thesis Collage of Education the University of Mustansiriyah, Baghdad, Iraq.
- Szilagy, M. (1988), "***Electron and Ion Optics***", Plenum Press: New York.
- Zipfel, B. (2006), "***3 1/2 - Dimensional Particle Interactive Optimisation***", Seventh International Conference on Charged Particle Optics (CPO-7), Abstract for Computer Software Demonstrations, Trinity College Junior Parlour.